Pergamon

0301-9322(95)00008-9

Int. J. Multiphase Flow Vol. 21, No. 5, pp. 721–732, 1995

0301-9322/95 $9.50 + 0.00

DYNAMIC VISCOUS RESUSPENSION OF BIDISPERSE SUSPENSIONS—I. EFFECTIVE DIFFUSIVITY

G. P. KRISHNAN and D. T. LEIGHTON JR

Department of Chemical Engineering, University of Notre Dame, Notre Dame, IN 46556, U.S.A.

(Received 9 May 1994; in revised form 26 January 1995)

Abstract—In this paper, we describe an experimental investigation into the dynamic viscous resuspension of bidisperse suspensions in an annular parallel plate device. We use the model of Chapman & Leighton to determine the effective diffusivity of the particulate phase (51.0 and 119.0 μm glass spheres) in the plane of shear as a function of overall concentration ($0.3 < \phi < 0.5$) as well as the relative size fraction of the large particles ($0.0 < \phi_L/(\phi_L + \phi_S) < 1.0$). The effective diffusivity of a mixed suspension was found to be somewhat less than the volume average of the diffusivities of monodisperse large and small sphere suspensions.

Key Words: suspensions, shear-induced diffusion, bidisperse, particulate forms

1. INTRODUCTION

The connection between suspension microstructure and observed rheological behavior is a fundamental problem in the study of suspensions. Properties such as the sedimentation rate, self-diffusion coefficient, effective diffusivity and viscosity have been investigated for monodisperse systems [a comprehensive review of this subject is provided by Roco (1993)], however the majority of industrially important suspensions are polydisperse in size or density. In polydisperse systems, the shear-induced interaction between the various species and their different sedimentation velocities pose a much more complex problem than the monodisperse systems previously investigated.

The effect of bidispersity on the rheological properties of concentrated suspensions has been studied by a number of workers. An extensive investigation into the variation of relative viscosity, in particular, was conducted by Chong *et al.* (1971) for suspensions over a concentration range of 54–74% by volume. They found that the relative viscosity of an (initially monodisperse) concentrated suspension decreased continuously with the addition of particles of a different size and reached a certain minimum value. At this point however, a further increase in the relative concentration of the second species caused the relative viscosity to increase and approach the value corresponding to a monodisperse suspension of the particles of the second kind. The influence of the particle size distribution on the variation of the relative viscosity was also recently investigated by Chang & Powell (1993) through Stokesian dynamics (Brady & Bossis 1989) numerical simulations. They found that the addition of smaller particles to a concentrated suspension ($\phi > 0.4$) tended to reduce the average cluster size resulting in a significant reduction in viscosity. Thus, not only is the overall concentration an important parameter but so is the relative concentration distribution of the two species in a bidisperse suspension. This is key to a complete understanding of the macroscopic behavior of bidisperse and polydisperse suspensions.

In investigating the rheology of bidisperse systems, two separate approaches are commonly used, namely: (a) direct visualization methods and (b) indirect methods in which rheological measurements are made on a rheometer, e.g. orifice, capillary, Couette or parallel-plate viscometers. In this paper, we describe our experimental observations made on an annular parallel plate viscometer to determine shear-induced diffusivity coefficients in the plane of shear. The dependence on the relative size fraction of large and small particles as well as the overall concentration will be examined.

The rheological behavior of bidisperse suspensions is studied by resuspending a suspension confined in an annular parallel plate viscometer. Resuspension is a process whereby a settled layer

of negatively buoyant spheres is entrained into the bulk fluid in the presence of an externally imposed shear flow. While such a phenomenon has been known to occur for flows with high Reynolds number (Thomas 1961), Gadala-Maria & Acrivos (1979) were the first to observe the same for systems in the absence of inertial forces. Leighton & Acrivos (1986) and Schaflinger *et al.* (1990) have attributed this to the diffusion of particles arising from irreversible interactions as a result of an imposed shear flow. This shear-induced migration phenomenon described by Leighton & Acrivos (1987b) has been used by Chapman & Leighton (1991) to develop a model for the transient variation of the relative viscosity of a monodisperse concentrated suspension during the resuspension process based on particle redistribution. Because of the strong dependence of viscosity on concentration, the torque signal observed during resuspension monotonically increases to an asymptotic value as the concentration profile becomes uniform. The rate of this increase can be used to measure the shear-induced effective diffusivity. The ratio of this shear-induced diffusivity to Brownian diffusivity scales as the Peclet number ($\dot{\gamma}\mu a^3/\kappa T$) which, for typical parameters used in experiments described here, is on the order of 10^8. Here, $\dot{\gamma}$ is the average shear-rate in the gap, μ is the viscosity of the suspension, a is the particle radius, κ the Boltzman constant and T the absolute temperature. Typical particle Reynolds numbers ($\dot{\gamma}a^2\rho/\mu$) in our experiments are on the order of 10^{-4}, ρ being the average density of the suspension, implying that inertial effects are similarly negligible.

A brief theoretical background relating the migration process to the increase in the measured torque signal is provided in the next section along the lines of Chapman & Leighton (1991). Section 3 contains a description of our experimental approach. Section 4 describes our results and the final section presents our conclusions.

2. THEORY

2.1. Resuspension of concentrated suspensions

To begin, consider a suspension of negatively buoyant (monodisperse) spheres undergoing a simple shear flow as depicted in figure 1. A sheared suspension of negatively buoyant particles experiences two counteracting fluxes (a) a downward sedimentation flux and (b) an upward shear-induced migration flux down concentration gradients (or shear rate). Hence, the time-dependent concentration distribution is governed by

$$\frac{\partial \phi}{\partial t} = \frac{\partial}{\partial y}\left[\frac{2}{9}\frac{\Delta\rho g a^2}{\mu_o} f\phi + D\frac{\partial \phi}{\partial y}\right] \qquad [1]$$

where ϕ is the volume fraction of particles, f is the hindrance to settling caused by the presence of other particles, μ_o is the viscosity of the pure suspending fluid, a is the particle radius, $g\Delta\rho$ is the buoyancy force and D is the shear-induced effective diffusivity within the plane of shear at constant shear-stress. This last quantity is closely related to the quantity $(K_\eta - K_c)(\phi^2/\mu)(\partial\mu/\partial\phi) + K_c\phi$ of the model proposed by Phillips *et al.* (1992), however the constant shear stress form of the diffusivity used here is more appropriate to resuspension flows since the shear stress is independent of position. This is the effective diffusivity measured by Leighton & Acrivos and Chapman & Leighton. At steady state, since the effective diffusivity is

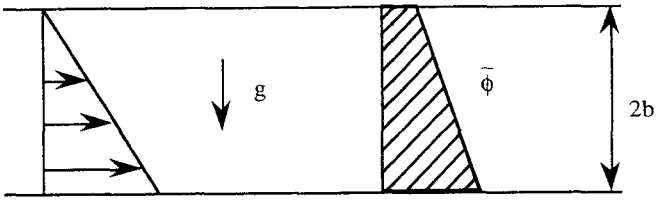

Figure 1. Experimental set-up showing a suspension of average concentration $\bar{\phi}$ subjected to a simple shear flow. The suspension experiences a downward sedimentation flux which is counteracted by an upward shear-induced migration flux.

proportional to the shear rate $\dot{\gamma} = \tau/(\mu_r \mu_o)$ where μ_r is the relative viscosity of the suspension, we obtain:

$$\frac{d\phi}{dy^*} = -\frac{2}{9}\left(\frac{b}{a}\right)\left[\frac{\Delta\rho g a}{\tau}\right]\left[\frac{f\phi\mu_r}{\hat{D}_\perp}\right] \quad [2]$$

where we have rendered y dimensionless with respect to the gap half-height b, and $\hat{D}_\perp = D_\perp/(\dot{\gamma}a^2)$ is the dimensionless effective diffusivity. Note that the dimensionless concentration gradient is inversely proportional to both the particle radius to gap half-height ratio a/b, and the Shields parameter $\Psi(\equiv \tau/\Delta\rho g a)$. For sufficiently large values of ψ and a/b the concentration gradient will be small and the profile will be approximately linear. Since the viscosity is a strong function of the concentration ϕ, the resultant torque signal is dependent on the concentration profile. Also, since the shear-stress is constant across the gap, we may define an observed relative viscosity for the suspension by:

$$\frac{1}{\mu_{r,obs}} = \frac{1}{2b}\int_{-b}^{b} \frac{1}{\mu_r}\, dy \quad [3]$$

If we expand the inverse relative viscosity in the gap as a Taylor series about the average concentration $\bar{\phi}$, we obtain:

$$\frac{1}{\mu_r} = \left|\frac{1}{\mu_r}\right|_{\bar{\phi}} + \left.\frac{\partial\left(\frac{1}{\mu_r}\right)}{\partial\phi}\right|_{\bar{\phi}}(\phi - \bar{\phi}) + \frac{1}{2}\left.\frac{\partial^2\left(\frac{1}{\mu_r}\right)}{\partial\phi^2}\right|_{\bar{\phi}}(\phi - \bar{\phi})^2 + O[(\phi - \bar{\phi})^3] \quad [4]$$

Substituting into [3] and noting that the average of $(\phi - \bar{\phi})$ across the gap is zero, we obtain:

$$\frac{|\mu_r|_{\bar{\phi}}}{\mu_{r,obs}} - 1 = \frac{1}{2}\left(\mu_r \left.\frac{\partial^2\left(\frac{1}{\mu_r}\right)}{\partial\phi^2}\right)\right|_{\bar{\phi}} \langle(\Delta\phi)^2\rangle + O\langle(\Delta\phi)^3\rangle \quad [5]$$

where $\Delta\phi$ is the deviation from the average concentration and brackets denote an average over the gap. Note that the viscosity function in [5] involves the second derivative of $1/\mu_r$. Chapman (1990) found that the reciprocal of the relative viscosity was very nearly a quadratic function of concentration and that the second derivative of the function was positive. This means that any fluctuation in concentration across the gap results in a decrease in the observed viscosity. Provided these concentration fluctuations are small (i.e. $\psi a/b$ is large), we can assume that the hindered settling factor f and the effective diffusivity $\hat{D}_\perp$ are approximately constant. We can thus solve the convective–diffusion equation together with the no-flux boundary condition to obtain the time-dependent concentration profile:

$$\phi(t^*, y^*) - \bar{\phi} = y^*\delta + \sum_{n=0}^{\infty} \frac{2\alpha(-1)^n}{(n+\frac{1}{2})^2\pi^2} \sin[(n+\tfrac{1}{2})\pi y^*] e^{-(n+(1/2))\pi^2\hat{D}_\perp t^*} \quad [6]$$

where the initial linear concentration profile is taken to be

$$\phi - \bar{\phi} = -\frac{2}{9}\left[\frac{1}{\Psi_L \frac{a}{b}}\right]\left[\frac{f\phi\mu_r}{\hat{D}}\right] y^* = -(\alpha + \delta) y^* \quad [7]$$

Here $t^* = t\gamma_H a^2/b^2$, $y^* = y/b$, ψ_L is the Shields parameter at the lower shear rate, ψ_H is the corresponding value at the higher shear rate, δ and $\alpha + \delta$ are the magnitudes of the concentration gradients at the higher and lower shear rates, respectively, and $\bar{\phi}$ is the average concentration in the gap. From [5] we can now obtain the transient relative viscosity variation. This can be approximated by

$$\frac{\frac{\mu_{r,obs}|_{t=\infty}}{\mu_{r,obs}} - 1}{\frac{\mu_{r,obs}|_{t=\infty}}{\mu_{r,obs}|_{t=0}} - 1} \approx \sum_{n=0}^{\infty} \frac{6}{(n+\frac{1}{2})^4\pi^4} \exp[-2(n+\tfrac{1}{2})^2\pi^2\hat{D}\, t^*] \quad [8]$$

provided $\delta/\alpha \ll 1$. This is achieved as $\psi_H a/b \to \infty$, a condition which was present during our experiments. For large values of $\psi_H a/b$ we can neglect the effects of gravity on the dynamics of the resuspension process itself. Gravity simply acts to set the initial condition for the resuspension process and thereafter plays no further role. Note that the relative viscosity is now only a function of the dimensionless diffusivity. A detailed description of the model described above is provided by Chapman (1990).

It is important to note that the theory described thus far is valid only for monodisperse suspensions. However, due to the lack of any corresponding model for polydisperse suspensions we have assumed that it holds for the bidisperse suspensions under investigation here. In fact, such an assumption is justified provided the particles of different size in the suspension remain well mixed at all times. This is likely to be reasonable approximation if the parameter $\psi_L a/b$ is sufficiently large. In our experiments, we examined the behavior of the resuspension process in the limit that $(\psi_L a/b)^{-1}$ approached zero. The diffusivity measured in such an experiment would thus be the average diffusivity of a well-mixed bidisperse suspension.

3. EXPERIMENTAL TECHNIQUE

3.1. Materials

Particles used in the experiments consisted of two size ranges of glass spheres. The glass spheres were two lots of Class V-A microbeads obtained from Ferro Corp. Cataphote Division, one of size 45–53 μm diameter and one size 106–125 μm diameter. Both lots were reported to be 90% in the listed size range. Actual measurement of the sizes of a large number of particles from each size range yielded average sizes and population standard deviations of 51.0 ± 3.8 and 119.0 ± 10.2 μm.

The glass particles were suspended in an 88 wt% solution of glycerin and water. The density of the large spheres was measured via water displacement and found to agree with the reported value of 2.42 g/cm^3. The glycerin–water solution had a density of 1.23 g/cm^3, thus the large spheres had a density difference of 1.19 g/cm^3. While the density of the small glass spheres was also reported to be 2.42 g/cm^3, it was measured to be 2.34 g/cm^3. The deviation in the densities between the two size lots was probably due to the larger volume percentage of air bubbles in the small spheres than in the large spheres. The viscosity of the suspending fluid was measured as a function of temperature on a CarriMed controlled stress rheometer and had a value of 1.62 p at 23.0°C. The temperature dependence of the pure fluid viscosity was important for accurate calculation of the suspension relative viscosity.

The suspensions were analyzed using an annular parallel plate viscometer with an outer diameter of 19.05 cm and an inner diameter of 14.05 cm yielding an aspect ratio of $(R_o - R_i)/R = 0.302$. This geometry yielded a shear stress which had a radial deviation from that at the average radius $\bar{R}$ of $\pm 15\%$. The annular plates were mounted on a Model R-18 Weissenberg Rheogoniometer equipped with a special clutch which allowed for switching between two drive motors operating at different rotational speeds. This clutch system resulted in a nearly instantaneous step change in shear rate.

3.2. Procedure

Well-mixed suspensions were loaded in the annular parallel plate viscometer by carefully pouring them around the surface of the lower plate. The upper plate was then lowered slowly until it contacted the suspension. When contact between the suspension and the upper plate was completed over 360°, the plate was lowered further until the gap between the plates was completely filled. By slowly rotating the bottom plate during the lowering of the upper plate and by placing a thin layer of Vaseline on the outer and inner edges of the plates, the problem of the leakage of suspension was circumvented. Through the rotation of the lower plate, a shear flow was produced in the gap between the lower and upper plates. The resultant torque on the upper plate was measured through the use of a transducer and a chart recorder. The observed relative viscosity was taken to be the ratio of the torque measured for a suspension to that measured for the pure suspending fluid in the same device with corrections for temperature and shear rate variations. In this way, most sources of systematic error in relative viscosity measurement were eliminated from the experiments.

Viscous resuspension was studied over a wide range of experimental conditions. Suspensions of glass spheres were studied over concentrations from 30 to 45%. Small and large particles were mixed in different proportions while keeping the overall concentration constant. Various degrees of bidispersity ranging from pure (100%) large spheres to pure (100%) small spheres were thus obtained.

The gap heights used for each experiment ranged from 1.8 to 2.8 mm. This resulted in particle diameter to gap height ratios ranging from 0.043 to 0.066 based on the large sphere size. For larger gaps, the suspensions had a tendency to leak out of the edges of the plates, therefore most experiments were performed at gaps of less than 2.5 mm. Suspensions were sheared at rates ranging from 0.6 to 180 s^{-1} depending on the concentration of the suspension. In general, as suspension concentration decreased (and hence the diffusivity as well), a higher shear rate was necessary to achieve resuspension. These shear rates gave rise to Shields parameters in the range of 6.0–53.0, which were sufficient to lead to a nearly uniform concentration profile at high shear and to avoid settling at low shear. The step changes in shear were by factors of $10^{0.7}$–$10^{1.4}$. These changes were adjusted to keep α and δ within acceptable parameter ranges. The temperature was monitored frequently during each experiment through the use of a digital thermometer with a probe attached to the top surface of the upper plate. This was then used to correct for thermal variations in the viscosity of the suspending fluid.

4. RESULTS

In this section, we present shear-induced diffusivity values for bidisperse suspensions of different concentrations measured from the transient variation of the relative viscosity when the suspension is subjected to a step-increase in shear rate. Figure 2 shows one such transient together with the viscosity variation predicted by the model described in section 2.1 for monodisperse suspensions. As can be seen, [8] fits the experimental data quite well, suggesting that the resuspending bidisperse suspension can be successfully modeled as a monodisperse suspension with some average particulate phase diameter. This was found to be true for all the experiments from which the effective diffusivity values presented in this section were determined.

The relative viscosity of the bidisperse suspensions used in our experiments was found to be a strong function of the relative size fraction of the species present. Figure 3 shows the variation of

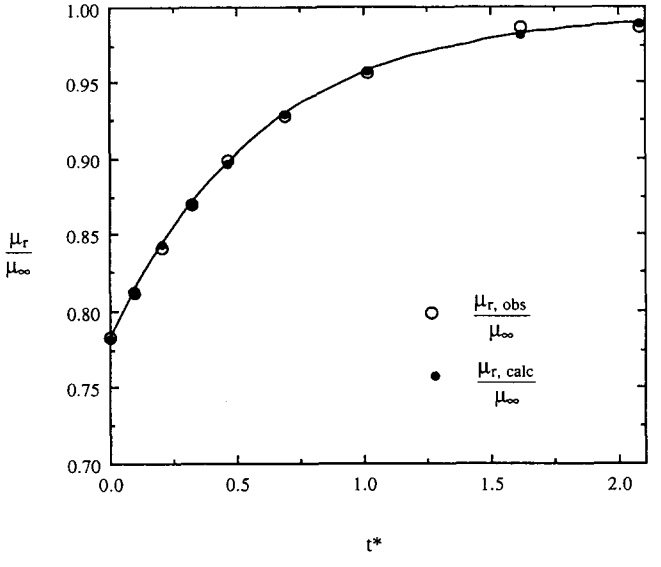

Figure 2. A typical transient behavior of the relative viscosity during the resuspension of a 40% concentration suspension containing equal amounts of large and small spheres. Low-shear shear rate is 5.256 s^{-1} and high-shear shear rate is 52.598 s^{-1}. Note the excellent agreement between the experimentally observed relative viscosity and the corresponding values predicted by [8].

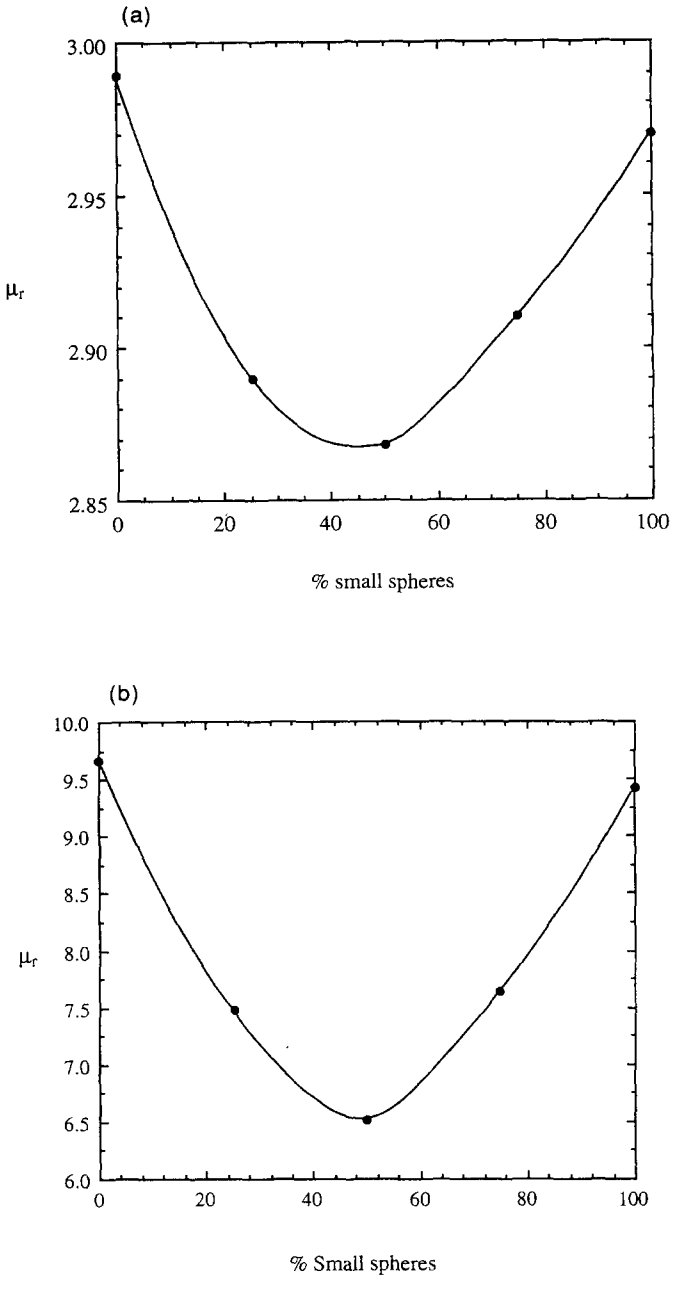

Figure 3(a) and (b). *Caption on facing page.*

the relative viscosity for the 30, 40 and 45% suspensions investigated in this study. As can be seen, the relative viscosity of a suspension containing a fixed volume fraction of spheres reached a minimum when equal amounts of the large and small spheres were present. These results are qualitatively similar to those of Chong *et al.* (1971).

The effective diffusivity of the suspensions was determined as a function of both the overall concentration and the relative size fractions of the individual species. The calculated values for the dimensionless diffusivities for different bidisperse suspensions are shown in figure 4 plotted as a function of $[(b)/(\psi_L \langle a \rangle)]^2$ where ψ_L is the Shields parameter at the lower shear rate and $\langle a \rangle$ is the average particle radius weighted with respect to the relative volume fraction of the different species of particles. In general, it is found that the calculated effective diffusivity is a slightly increasing

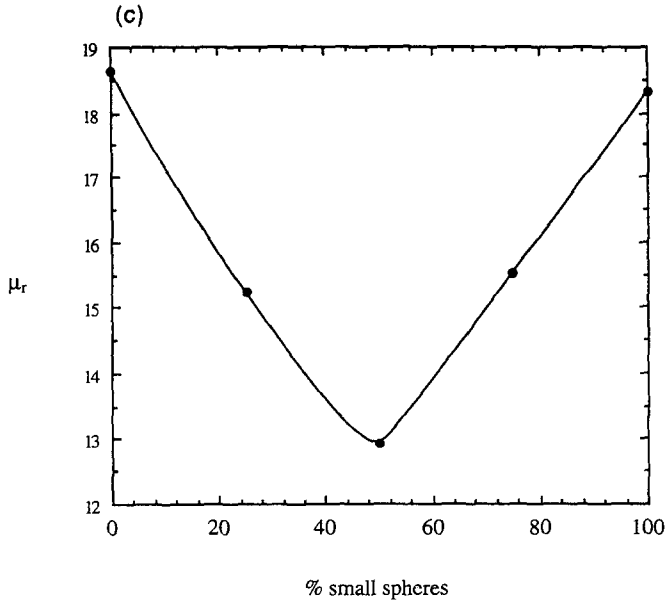

Figure 3(c)

Figure 3(a). Relative viscosity variation with bidispersity for 30% concentration suspensions. All measurements were made between shear rates of 93.29 and 104.50 s^{-1}. (b) Relative viscosity variation with bidispersity for 40% concentration suspensions. All measurements were made between shear rates of 34.21 and 41.43 s^{-1}. (c). Relative viscosity variation with bidispersity for 45% concentration suspensions. All the measurements were made between shear rates of 35.40 and 45.12 s^{-1}.

function of $[(b)/(\psi_L\langle a\rangle)]^2$. As the lower shear rate is decreased (i.e. $[(b)/(\psi_L\langle a\rangle)]^2$ is increased), one might expect an increase in the degree of segregation in the gap. Under those conditions, the assumptions made during the derivation of [8] that the two species are well mixed and that the total concentration gradient in the gap is small will no longer be correct. Further, at lower shear rates the sedimentation flux may result in a higher perceived diffusion coefficient. Note that all the diffusivities in figure 4 are non-dimensionalized with respect to $\dot{\gamma}_L\langle a\rangle^2$ where $\langle a\rangle$ is the volume-averaged particle radius.

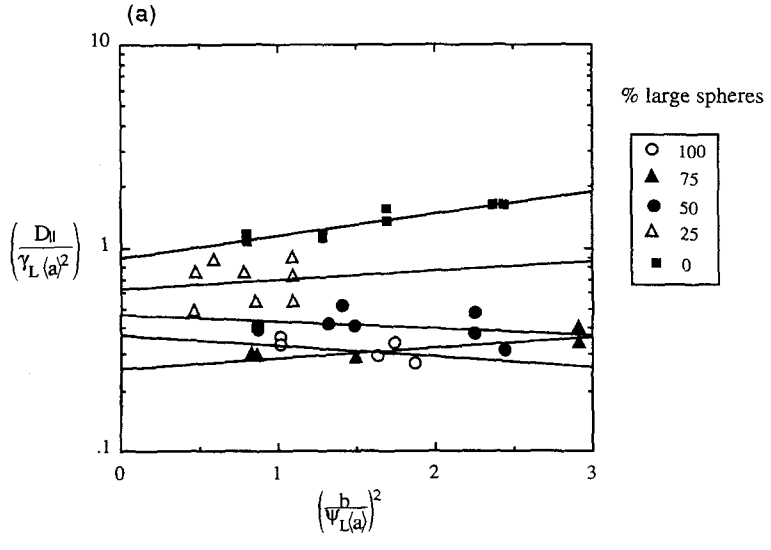

Figure 4(a). *Caption on p. 729*

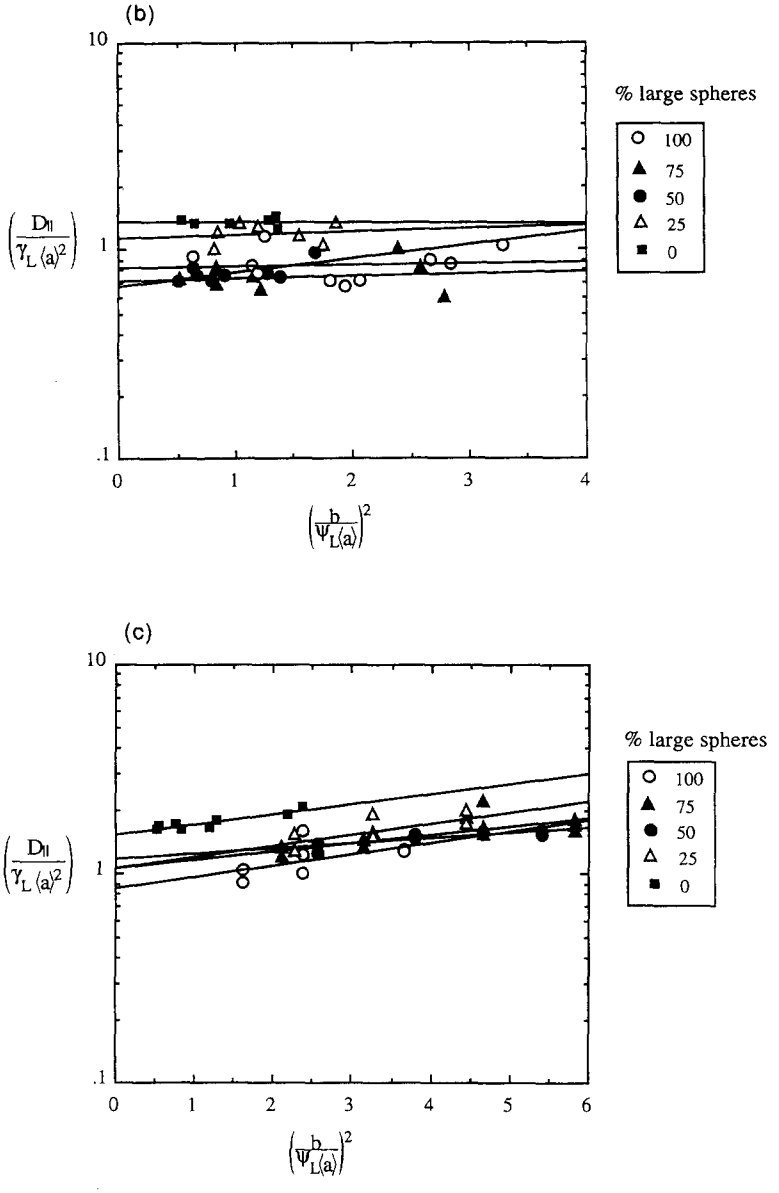

Figure 4(b) and (c). *Caption on facing page.*

The calculation of the diffusivity is prone to error from a number of sources most of which are associated with the experimental procedure itself. Some of these are (a) entrainment of air-bubbles in the suspension, (b) polydispersity in the $\langle 51.0\rangle$ μm and $\langle 119.0\rangle$ μm particles that were used to make the suspensions, (c) variation of the shear stress across the width of the annular region confining the suspension which is about $\pm$ 15% and (d) error in digitizing the transient response of the relative viscosity from which the diffusivities are calculated. Because of the complicated dependence of the effective diffusivity on each of these factors, it is difficult to determine the overall magnitude of the error in the measurements. A rough estimate, apparently justified by the reproducibility of the measurements after corrections for temperature and suspending fluid viscosity have been made, is about 15%. The diffusivity measurements at the higher concentrations showed less scatter and a more definite variation with ψ_L.

In order to obtain the value of the effective diffusivity corresponding to a well-mixed suspension, we look at the asymptotic behavior for large values of the Shields parameter. The extrapolated values of the effective diffusivity for $[(b)/(\psi_L\langle a\rangle)]^2 \to 0$ for all the systems investigated together with

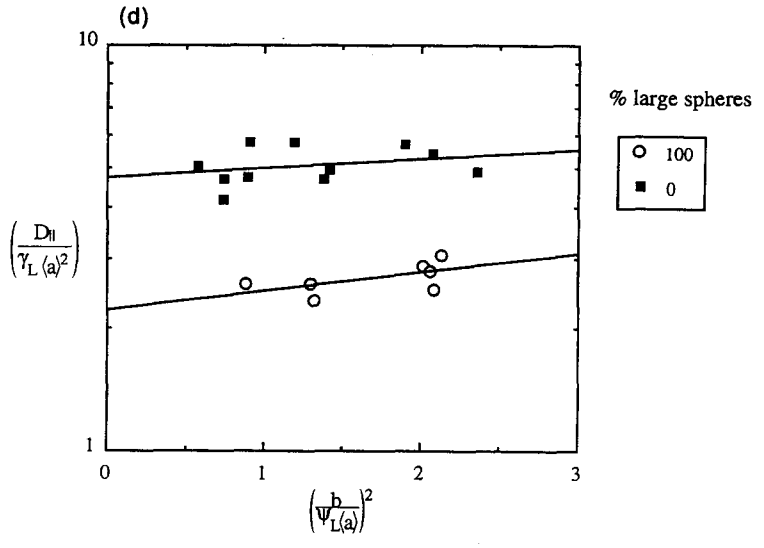

Figure 4(d)

Figure 4. (a) Dimensionless effective diffusivity for 30% concentration bidisperse suspensions. Note the large degree of scatter arising due to a small observable increase in the torque signal upon resuspension. (b) Dimensionless effective diffusivity for 40% concentration bidisperse suspensions. (c) Dimensionless effective diffusivity for 45% concentration bidisperse suspensions. (d) Dimensionless effective diffusivity for 50% concentration monodisperse suspensions. Due to the strong influence of particle segregation on the relative viscosity at higher concentrations, diffusivity data could not be obtained by fitting the experimentally observed torque signal for bidisperse suspensions to [8].

1σ error bars estimated from the scatter in the observations are shown in figure 5. Note that as the overall concentration of the bidisperse suspensions is decreased, so is the effective diffusivity. The large scatter in the low concentration measurements was principally the result of the lower magnitude of the torque signal increase upon resuspension at these concentrations.

The dimensionless diffusivities for a monodisperse suspension of the small spheres (average diameter 5.1 μm) were always larger than those observed for the other suspensions, a trend that was also observed by Chapman (1990). While the exact reason for such behavior is still unknown,

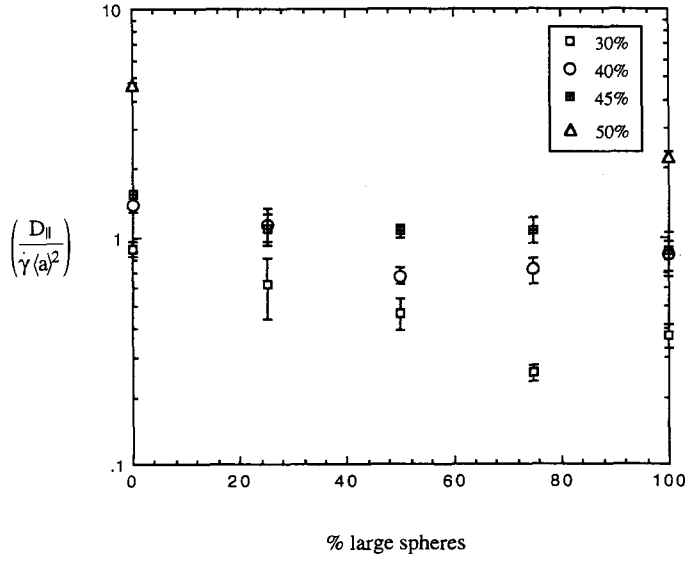

Figure 5. Extrapolated diffusivity values with 1σ error bars for $[(b)/(\Psi_L \langle a \rangle)]^2$ tending to zero. Note the increase in the dimensionless diffusivity as the fraction of small spheres is increased.

we suggest a few possible explanations: (a) the shear-induced diffusivities scale as some power of the particle radius other than 2, although it is difficult to see how this could occur from dimensional arguments. (b) Leighton & Acrivos have suggested irreversible non-hydrodynamic interactions such as those due to surface roughness effects as a possible mechanism for shear-induced diffusion. The dimensionless roughness for the small glass spheres was observed in the experiments of Smart & Leighton (1989) to be about twice that of the large particles. This could account for the larger dimensionless effective diffusivity for the smaller particles. (c) Yet another possibility is that the smaller particles tend to form aggregates in the presence of the suspending fluid used in our experiments resulting in a larger effective particle size and hence a larger diffusivity. Note that we have no experimental evidence that this occurred.

Under certain conditions of low Shields parameter, it was found that the torque signal observed upon resuspension did not monotonically increase to a steady state value, but rather went through a maximum at some finite strain (figure 6). Subsequent to this, the torque signal (relative viscosity) decayed exponentially to reach a steady state value. The time scale associated with the initial increase was consistent with the resuspension time scale of other experiments in which the phenomenon was absent and found to be much shorter than that associated with the subsequent decrease. The overshoot was predominant at higher concentrations, particularly the 50% bidisperse suspensions. For these suspensions, it was found that the overshoot persisted for all low-shear shear rates until a value of Ψ_L was reached where the suspension had completely resuspended. For this reason no values for the effective diffusivity of bidisperse suspensions at this concentration are reported. The 40% bidisperse suspensions also exhibited this overshoot behavior at sufficiently low shear rates. Unlike the 50% suspensions however, the overshoot vanished at values of low-shear Shields parameters where the suspension was not completely resuspended, and thus diffusivity measurements could be made. No overshoot behavior was observed for monodisperse suspensions. Because this overshoot phenomenon was associated with low values of $\psi_L a/b$ and was absent for monodisperse suspensions it was attributed to particle size segregation at low shear rates. This phenomenon must be resolved by future direct flow visualization studies. Segregation behavior has also been observed by Graham *et al.* (1991) in suspensions of bidisperse particles in a wide-gap Couette geometry.

5. CONCLUSIONS

We have conducted dynamic viscous resuspension experiments with bidisperse suspensions and determined shear-induced diffusion coefficients as a function of both bidispersity and overall concentration. Note that in the results presented earlier, the effective diffusivities have been non-dimensionalized with respect to the volume averaged particle radius. An alternative way of

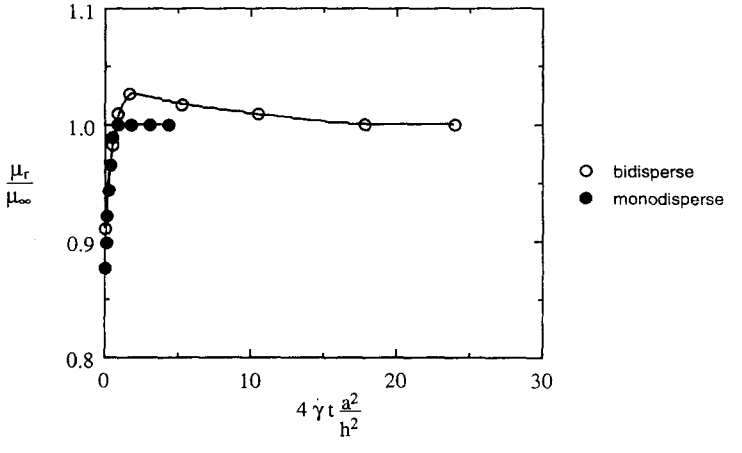

Figure 6. Comparison of bidisperse and monodisperse suspensions. Both suspensions were subjected to a low shear shear rate of 6.32 s^{-1}. Note that the monodisperse suspension of large spheres exhibited no stress overshoot.

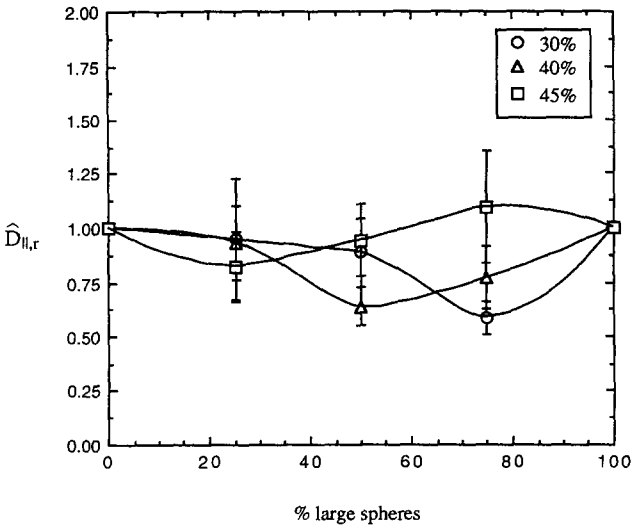

Figure 7. Dimensionless effective diffusivity with 1σ error bars for the various suspensions investigated. $\hat{D}_{\|,r}$ is the effective diffusivity $D_{\|}$ non-dimensionalized with respect to the volume averaged diffusivity of the monodisperse suspensions.

examining the effect of bidispersity on the effective diffusivity is to normalize the diffusivity by the volume average of the measured diffusivities for monodisperse large and small spheres denoted by $D_{\|,L}$ and $D_{\|,S}$ respectively. This effectively uses a mean-squared particle radius for the bidisperse suspension as opposed to a volume averaged one. Thus we let this reduced diffusivity be given by:

$$\hat{D}_{\|,r} = \frac{D_{\|}}{(x_L D_{\|,L} + x_S D_{\|,S})} \qquad [9]$$

where x_L and x_S are the relative volume fractions $\phi_L/(\phi_L + \phi_S)$ and $\phi_S/(\phi_L + \phi_S)$ of the large and small spheres, respectively. This has the effect of eliminating the bias towards smaller spheres in figure 5 due to the larger observed dimensionless diffusivity for monodisperse small sphere suspensions. A plot of this reduced diffusivity versus the fraction of large spheres is made in figure 7 with 1σ error bars. As can be seen by comparison with figure 3, the reduced diffusivity, as is the case with the relative viscosity, is somewhat smaller than that for the monodisperse suspensions at the same concentration. The packing effect on the reduced diffusivity at high concentrations is somewhat less than that on the viscosity, however the magnitude and location of the minimum is probably not statistically significant due to the scatter in the diffusivity measurements. Therefore, from these experiments it has not been possible to resolve the issue of the appropriate average particle radius to use while non-dimensionalizing the effective diffusivities.

Acknowledgement—This work was funded in part by a grant from Lockheed Missiles & Space Inc.

REFERENCES

Abott, J. R., Tetlow, N., Graham, A. L., Altobelli, S. A., Fukushima, E., Mondy, L. A & Stephens, T. S. 1991 Experimental observations of particle migration in concentrated suspensions: Couette flow. *J. Rheol.* **35,** 773–795.

Brady, J. F. & Bossis, G. 1989 Stokesian dynamics. *A. Rev. Fluid Mech.* **20,** 111–157.

Chang, C. & Powell, R. L. 1993 Dynamic simulation of bimodal suspensions of hydrodynamically interacting spherical particles. *J. Fluid. Mech.* **253,** 173–209.

Chapman, B. K. 1990 Shear induced migration phenomena in concentrated suspensions. Ph. D. thesis, University of Notre Dame, Notre Dame, IN.

Chapman, B. K. & Leighton, D. T. 1991 Dynamic viscous resuspension. *Int. J. Multiphase Flow* **17,** 469–483.

Chong, J. S., Christiansen, E. B. & Baer, A. D. 1971 Rheology of concentrated suspensions. *J. Appl. Polym. Sci.* **15,** 2007–2021.

Gadala-Maria, F. & Acrivos, A. 1979 Shear-induced structure in a concentrated suspension of solid spheres. *J. Rheol.* **24,** 799–814.

Graham, A. L., Altobelli, S. A., Fukushima, E., Mondy, L. A. & Stephens, T. S. 1991 Note: NMR imaging of shear-induced diffusion and structure in concentrated suspensions undergoing Couette flow. *J. Rheol.* **35,** 191–201.

Leighton, D. T. & Acrivos, A. 1987a Measurement of shear-induced self-diffusion in concentrated suspensions of spheres. *J. Fluid Mech.* **177,** 109–131.

Leighton, D. T. & Acrivos, A. 1987b The shear-induced migration of particles in concentrated suspensions. *J. Fluid Mech.* **181,** 415–439.

Phillips, R. J., Armstrong, R. C., Brown, R. A., Graham, A. L. & Abbot, J. R. 1992 A constitutive equation for concentrated suspensions that accounts for shear-induced particle migration. *Phys. Fluids A* **4,** 30.

Roco, M. C. (Ed.) 1993 *Particulate Two-phase Flow*. Butterworth–Heinemann, Oxford.

Schaflinger, U., Acrivos, A. & Zhang, K. 1990 Viscous resuspension of a sediment within a laminar and stratified flow. *Int. J. Multiphase Flow* **16,** 567–578.

Smart, J. R. & Leighton, D. T. 1989 Measurement of the hydrodynamic surface roughness of noncolloidal spheres. *Phys. Fluids A* **1,** 52–60.

Thomas, D. G. 1961 Transport characteristics of suspensions: II. Minimum transport velocity for flocculated suspensions in horizontal pipes. *AIChE Jl* **7,** 423–430.